

An Approximate Maximum Likelihood Time Synchronization Algorithm for Zero-padded OFDM in Channels with Impulsive Gaussian Noise

Koosha Pourtahmasi Roshandeh, *Student Member, IEEE*, Mostafa Mohammadkarimi, *Member, IEEE*, and Masoud Ardakani, *Senior Member, IEEE*

Abstract—In wireless communication systems, Orthogonal Frequency-Division Multiplexing (OFDM) includes variants using either a cyclic prefix (CP) or a zero padding (ZP) as the guard interval to avoid inter-symbol interference. OFDM is ideally suited to deal with frequency-selective channels and additive white Gaussian noise (AWGN); however, its performance may be dramatically degraded in the presence of impulse noise. While the ZP variants of OFDM exhibit lower bit error rate (BER) and higher energy efficiency compared to their CP counterparts, they demand strict time synchronization, which is challenging in the absence of pilot and CP. Moreover, on the contrary to AWGN, impulse noise severely corrupts data. In this paper, a new low-complexity timing offset (TO) estimator for ZP-OFDM for practical impulsive-noise environments is proposed, where relies on the second-order statistics of the multipath fading channel and noise. Performance comparison with existing TO estimators demonstrates either a superior performance in terms of lock-in probability or a significantly lower complexity over a wide range of signal-to-noise ratio (SNR) for various practical scenarios.

I. INTRODUCTION

OFDM technique is widely employed in wireless communications, mainly due to its ability in converting a frequency-selective fading channel into a group of flat-fading sub-channels [1]. Compared to conventional single-carrier systems, OFDM offers increased robustness against multipath fading distortions since channel equalization can be easily performed in the frequency domain through a bank of one-tap multiplier [2]. Moreover, OFDM can be efficiently implemented using fast Fourier transform (FFT) [3], which makes it more appealing compared to other multi-carrier modulation techniques such as Filter Bank Multi Carrier and Generalised Frequency Division Multiplexing.

Owing to superior advantages of OFDM, it is exploited in many IEEE standards, such as, IEEE 802.15.3a, IEEE 802.16d/e, and IEEE 802.15.4g [4]–[6], which are used for different applications. For instance, OFDM combined with massive multiple-input multiple-output (MIMO) technique achieves a high data rate, making it suitable for multimedia broadcasting [7]. Moreover, many Internet of Things (IoT) applications such as smart buildings and Vehicle-to-everything (V2X) leverage OFDM as their main communication scheme [6], [8].

OFDM, however, undergoes a severe inter symbol interference (ISI) caused by the high selectivity of the fading channel

[9]. In order to mitigate this issue, usually a guard interval with a fixed length is inserted between every two consecutive OFDM symbols. When the guard interval is the partial repetition of the transmitting data samples, this scheme is called CP-OFDM [10]. The primary benefit of CP-OFDM is the ease of TO estimation or equivalently estimating the starting point of FFT. This is referred to as time synchronization [11], and is easily carried out by using CP and its correlation with the data sequence. Despite the ease of time synchronization in CP-OFDM, it possesses some major disadvantages such as excessive power transmission which is due to the transmission of CP. ZP-OFDM [12], where the guard interval is filled with zeros, overcomes this issue. However, the time synchronization, or equivalently TO estimation, in ZP-OFDM becomes a very difficult and complicated task.

There are two approaches in order to estimate TO in ZP-OFDM. In the first approach which is called data-aided (DA) time synchronization, a series of training sequences (pilots) are used to estimate TO. The second approach, referred to as non-data-aided (NDA) time synchronization, however, relies on the statistical properties of the transmitted data sequence.

A. Related work

The DA time synchronization for ZP-OFDM has been studied in the literature [13]. On the other hand, NDA time synchronization lacks a reliable mathematical analysis. An NDA time synchronization algorithm for ZP-OFDM has been proposed in [14], [15] which are mainly heuristic algorithms. More specifically, these algorithms trace the energy ratio of partially cropped data sequences; which do not always show a reliable performance in terms of lock-in probability for highly selective channels. Also, a mathematical approach towards NDA TO estimation for ZP-OFDM systems has been proposed in [16]. The authors in [16] proposed a maximum likelihood (ML) TO estimator for a ZP-OFDM under a frequency selective channel. However, the algorithm in [16] is highly complex which hinders its implementation for MIMO systems. Moreover, the algorithm proposed in [16] is designed for AWGN channel which implies that its performance degrades when the channel experiences an impulsive noise.

B. Motivation

ZP-OFDM requires less transmission power compared to CP-OFDM, due to lack of CP, which makes it a suitable can-

didate for future IoT devices. However, time synchronization becomes challenging in ZP-OFDM where time synchronization algorithms fail to achieve high lock-in probability, or are highly complex for practical implementations. Moreover, the proposed TO estimators for ZP-OFDM systems so far are developed for Gaussian noise models. However, many real-world channels, e.g. underwater, urban and indoor channels, are known to experience an impulsive noise, rather than a simple Gaussian noise [17]–[20]. This noise is originally coming from the great amount of noise in the nature, and the electronic equipment. It is well-known that designing communication systems under simple Gaussian noise model can significantly affect the performance of such systems when they experience an impulsive noise in reality [21]. Hence, an accurate yet low-complex time synchronization algorithm for ZP-OFDM are still needed to be developed.

In this paper, we propose a low complexity mathematical approach towards NDA time synchronization for ZP-OFDM systems in an impulsive noise channel. Simulation results demonstrate that the proposed estimator has a negligible performance gap in terms of lock-in probability with the estimator in [16] while possessing a significantly lower complexity.

C. Contributions

In this paper, we

- propose a low-complexity approximate ML TO estimator for MIMO ZP-OFDM systems in highly selective channels with impulsive noise. This algorithm (i) achieves high lock-in probability, and (ii) has significantly lower complexity compared to [16].
- Higher order statistics of the proposed approximate probability density function (PDF) of the received samples are investigated.
- A lower complexity algorithm, i.e. Energy Detector (ED), for MIMO ZP-OFDM systems experiencing Gaussian noise is proposed. This algorithm achieves high lock-in probability for high SNRs while possessing a low complexity.
- Complexity of the proposed algorithms and the one in [16] has been studied.

The paper is organized as follows. System model is discussed in Section II. The main ideas and the proposed ML estimator for systems are presented in Section III. The complexity of the algorithm is compared to that of proposed in [16] is studied in Section IV. Simulation results and conclusions are given in Sections V and VI, respectively.

Notations: Column vectors are denoted by bold lower case letters. Random variables are indicated by uppercase letters. Matrices are denoted by bold uppercase letters. Conjugate, absolute value, transpose, and the expected value are indicated by $(\cdot)^*$, $|\cdot|$, $(\cdot)^T$, and $\mathbb{E}\{\cdot\}$, respectively. Brackets, e.g. $\mathbf{a}[k]$, are used for discrete indexing of a vector \mathbf{a} .

II. SYSTEM MODEL

We consider a MIMO-OFDM wireless system with m_t and m_r transmit and receive antennas, respectively. This

system uses ZP-OFDM technique to communicate over a frequency selective Rayleigh fading channel. We assume a perfect synchronization at the transmit antennas. Let $\{x_k^{(n)}\}_{k=0}^{n_x-1}$, $\mathbb{E}\{|x_k|^2\} = \sigma_x^2$ be the n_x complex data samples from the n -th OFDM block to be transmitted from the i -th transmit antenna. Hence, their corresponding OFDM signal can be expressed as

$$x_i^{(n)}(t) = \sum_{k=0}^{n_x-1} x_k^{(n)} e^{\frac{j2\pi kt}{T_x}} \quad 0 \leq t \leq T_x, \quad (1)$$

where T_x denotes the duration of the data signal. To deal with the delay spread of the wireless channel, a zero-padding guard interval of length T_z is added to (1), in order to form the transmitted OFDM signal. Hence, the n -th transmitted OFDM signal from the i -th transmit antenna is given as

$$s_i^{(n)}(t) = \begin{cases} x_i^{(n)}(t) & 0 \leq t \leq T_x \\ 0 & T_x < t \leq T_s, \end{cases} \quad (2)$$

where T_s denotes the signal duration, and $T_s = T_x + T_z$.

Since the receiver demodulates the received signal and performs sampling, it is more convenient from both practical and mathematical point of view to develop algorithms and perform the analysis in baseband and discrete format. To this end, we continue our analysis in discrete baseband format from now on.

Let us denote the sampling rate at the receiver by $f_s = 1/T_{sa}$. We assume the transmitted signal, i.e. $s_i^{(n)}(t)$, passes through a frequency selective channel with n_h -taps. Let $\{h_{ji}[k]\}_{k=0}^{n_h-1}$ denote the k -th channel tap between the transmit antenna i and the received antenna j . The channel taps are assumed to be statistically independent complex Gaussian random variables with zero-mean, i.e. Rayleigh fading. The delay profile of the taps are given as

$$\mathbb{E}\{h[k]h^*[k-m]\} = \sigma_{h_k}^2 \delta[m], \quad (3)$$

$k = 0, 1, \dots, n_h - 1$. We assume the channel delay profile is known to the receiver.

In the absence of synchronization error and ISI, the discrete received baseband vector is expressed as

$$\mathbf{Y}^{(n)} = \begin{cases} \mathbf{H}\mathbf{S}^{(n)} + \mathbf{W}^{(n)}, & n \geq 0 \\ \mathbf{W}^{(n)}, & n < 0, \end{cases} \quad (4)$$

where \mathbf{H} denotes the discrete channel filter, and is defined as

$$\mathbf{H} = \begin{pmatrix} H_{11} & H_{12} & \cdots & H_{1m_t} \\ H_{21} & H_{22} & \cdots & H_{2m_t} \\ \vdots & \cdots & \ddots & \cdots \\ H_{m_r 1} & H_{m_r 2} & \cdots & H_{m_r m_t} \end{pmatrix} \quad (5)$$

where H_{ji} is the lower triangular Toeplitz channel matrix between transmit antenna i and the received antenna j , with

first column $[h_{ji}[0] \ h_{ji}[1] \ \dots \ h_{ji}[n_h - 1] \ 0 \ \dots \ 0]^T$. We set this matrix to be $n_s \times n_s$ where

$$\begin{aligned} n_s &= n_x + n_z, & n_s &\triangleq T_s/T_{sa} \\ n_x &\triangleq T_x/T_{sa}, & n_z &\triangleq T_z/T_{sa} \end{aligned} \quad (6)$$

where n_s , n_x , and n_z denote the number of OFDM signal samples, number of data samples, and the number of zero samples, respectively. Moreover, $\mathbf{S}^{(n)}$, $\mathbf{Y}^{(n)}$, and $\mathbf{W}^{(n)}$ are defined as

$$\mathbf{S}^{(n)} = \begin{pmatrix} \mathbf{s}_1^{(n)} \\ \mathbf{s}_2^{(n)} \\ \vdots \\ \mathbf{s}_{m_t}^{(n)} \end{pmatrix}, \quad \mathbf{Y}^{(n)} \triangleq \begin{pmatrix} \mathbf{y}_1^{(n)} \\ \mathbf{y}_2^{(n)} \\ \vdots \\ \mathbf{y}_{m_r}^{(n)} \end{pmatrix}, \quad \mathbf{W}^{(n)} \triangleq \begin{pmatrix} \mathbf{w}_1^{(n)} \\ \mathbf{w}_2^{(n)} \\ \vdots \\ \mathbf{w}_{m_r}^{(n)} \end{pmatrix} \quad (7)$$

where $\mathbf{y}_j^{(n)}$, $\mathbf{w}_j^{(n)}$, and $\mathbf{s}_i^{(n)}$ denote the received vector at the j -th receive antenna, the noise vector at the j -th receive antenna, and the transmitted vector from the i -th transmit antenna, respectively, and are given as

$$\mathbf{y}_j^{(n)} \triangleq [y_j^{(n)}[0] \ y_j^{(n)}[1] \ \dots \ y_j^{(n)}[n_s - 1]]^T \quad (8)$$

$$\mathbf{w}_j^{(n)} \triangleq [w_j^{(n)}[0] \ w_j^{(n)}[1] \ \dots \ w_j^{(n)}[n_s - 1]]^T \quad (9)$$

$$\begin{aligned} \mathbf{s}_i^{(n)} &\triangleq [s_i^{(n)}[0] \ s_i^{(n)}[1] \ \dots \ s_i^{(n)}[n_s - 1]]^T \\ &= [x_i^{(n)}(0) \ x_i^{(n)}(T_{sa}) \ \dots \ x_i^{(n)}((n_x - 1)T_{sa}) \ \underbrace{0 \ \dots \ 0}_{n_z}]^T \end{aligned} \quad (10)$$

Note that if the receiver starts to receive samples before any data is transmitted, it only receives noise samples, thus, we have $\mathbf{Y}^{(n)} = \mathbf{W}^{(n)}$, $n < 0$ in (4). In order to avoid ISI, the length of the zero-padding should be greater than or equal to the number of channel taps, i.e. $n_z \geq n_h$. This assumption holds throughout our analysis in this paper. We also consider the Class A impulsive noise model, i.e. Gaussian mixtures, that is defined as [22]

$$f_{W_j^{(n)}[k]}(w) = \sum_{l=0}^{L-1} p_l \mathcal{CN}(w : 0, \sigma_{w_l}^2), \quad (11)$$

for $k \in \{0, 1, \dots, n_s - 1\}$. It is well-known that the Gaussian mixture noise is a more accurate noise model than the conventional simple Gaussian model [21]. That is, the Gaussian mixture distribution models the noise in many real-world channels such as urban, underwater, and indoor channels, more accurately compared to the conventional simple Gaussian model [17]–[20].

According to the Central Limit Theorem (CLT), transmitted OFDM samples, i.e. $s_i^{(n)}[k] = x_i^{(n)}(kT_{sa})$, $\forall k \in \{0, 1, \dots, n_x - 1\}$, can be modeled as independent and identically distributed (i.i.d) zero-mean Gaussian random variables. Hence,

$$s_i^{(n)}[k] \text{ or } x_i^{(n)}(kT_{sa}) \sim \mathcal{CN}(0, \sigma_x^2), \quad \forall k \in \{0, 1, \dots, n_x - 1\} \quad (12)$$

where

$$\mathbb{E}\{s_i^{(n)}[k]s_p^{(n)}[k']^*\} = \mathbb{E}\{x_i^{(n)}(kT_{sa})x_p^{(n)}(k'T_{sa})^*\} \quad (13)$$

$$= \sigma_x^2 \delta[k - k'] \delta[i - p], \quad (14)$$

$$\forall i, p \in \{1, 2, \dots, m_t\},$$

$$\forall k, k' \in \{0, 1, \dots, n_x - 1\}.$$

Now, assume that there is a TO $\tau \triangleq dT_{sa} + \epsilon$ between the transmitter and the receiver, where d and ϵ represent the integer and fractional part of the TO, respectively. Since the fractional part of TO, ϵ , can be corrected through channel equalization, it suffices to estimate the beginning of the received OFDM vector within one sampling period. In fact, it is common in practice to model the TO as a multiple of the sampling period, and consider the remaining fractional error as part of the channel impulse response. To this end, we focus on estimating the integer part of the TO, d , which is essential in order to perform the FFT operation at the receiver, and decode the data in subsequent steps.

The next sections propose an approximate ML estimator for estimating d .

III. MAXIMUM LIKELIHOOD ESTIMATION FOR SINGLE-INPUT SINGLE-OUTPUT SYSTEM

In order to better understand the main ideas, and for the sake of notation simplicity, we first derive the approximate ML TO estimator for a single-input single-output (SISO)-OFDM system where $m_t = 1$ and $m_r = 1$. We then extend the proposed results for SISO systems in order to obtain the ML TO estimator for MIMO-OFDM systems.

We consider a SISO wireless system; hence, $m_t = 1$ and $m_r = 1$. For the sake of notation simplicity, we remove the subscripts i or j , denoting the variables associated with the i -th transmit or j -th receive antenna, from $\mathbf{y}_j^{(n)}$, $y_j^{(n)}[k]$, $\mathbf{w}_j^{(n)}$, $w_j^{(n)}[k]$, $\mathbf{s}_i^{(n)}$, $s_i^{(n)}[k]$, H_{ji} , $h_{ji}[k]$, and $x_i^{(n)}(k)$. Hence, Equation (4) can be rewritten as

$$\mathbf{y}^{(n)} = \begin{cases} \mathbf{H}\mathbf{s}^{(n)} + \mathbf{w}^{(n)} \triangleq \mathbf{v}^{(n)} + \mathbf{w}^{(n)}, & n \geq 0 \\ \mathbf{w}^{(n)}, & n < 0 \end{cases} \quad (15)$$

where

$$\mathbf{y}^{(n)} \triangleq [y^{(n)}[0] \ y^{(n)}[1] \ \dots \ y^{(n)}[n_s - 1]]^T \quad (16)$$

$$\mathbf{v}^{(n)} \triangleq [v^{(n)}[0] \ \dots \ v^{(n)}[1] \ \dots \ v^{(n)}[n_s - 1]]^T \quad (17)$$

$$\mathbf{w}^{(n)} \triangleq [w^{(n)}[0] \ \dots \ w^{(n)}[1] \ \dots \ w^{(n)}[n_s - 1]]^T \quad (18)$$

$$\begin{aligned} \mathbf{s}^{(n)} &\triangleq [s^{(n)}[0] \ s^{(n)}[1] \ \dots \ s^{(n)}[n_s - 1]]^T \\ &= [x^{(n)}(0) \ x^{(n)}(T_{sa}) \ \dots \ x^{(n)}((n_x - 1)T_{sa}) \ \underbrace{0 \ \dots \ 0}_{n_z}]^T. \end{aligned} \quad (19)$$

and \mathbf{H} is the lower triangular $n_s \times n_s$ Toeplitz channel matrix with first column $[h[0] \ h[1] \ \dots \ h[n_h - 1] \ 0 \ \dots \ 0]^T$.

Now, we assume that the integer part of the TO, d , can take values from a set $\mathcal{D} = \{-n_s + 1, \dots, -1, 0, 1, \dots, n_s - 1\}$, i.e. $d \in \mathcal{D}$. Note that the negative values of the delay, d , denotes the time when the receiver starts early to receive samples. That

is, for $d < 0$, the receiver receives $|d|$ noise samples from the environment, and then receives the transmitted OFDM samples starting from the $|d| + 1$ -th sample at the receiver. Similarly, when $d \geq 0$, the receiver starts late to receive the samples. In other words, the receiver misses the first d samples from the transmitted OFDM samples. Allowing d to take both negative and positive values enables the final estimator to perform both the frame and symbol synchronization; hence, it possesses a significant advantage.

The problem of estimating the TO can be formulated as a multiple hypothesis testing problem, i.e. $H_d, \forall d \in \mathcal{D} = \{-n_s + 1, \dots, n_s - 1\}$. We first assume that the receiver uses N observation vectors, $\mathbf{y}^{(0)}, \mathbf{y}^{(1)}, \dots, \mathbf{y}^{(N-1)}$, each with length n_s , in order to estimate the timing offset d . Later, we allow the receiver to use any arbitrary number of received samples, not necessarily a multiple of n_s , for estimation. In order to derive the ML TO estimator, we need to obtain the joint PDF of the N observation vectors under the different hypotheses H_d . Assuming H_d , this PDF is denoted by $f(\mathbf{y}^{(0)}, \mathbf{y}^{(1)}, \dots, \mathbf{y}^{(N-1)} | H_d)$.

The following lemma from [16] gives some insights about the samples of the received vectors. We provide this lemma here without the proof.

Lemma 0.1. *For any arbitrary n and k , $0 \leq k \leq n_s - 1$, let us define the actual index of an observation sample, i.e. $y^{(n)}[k]$, as $k^{\text{ac}} = n_s n + k$. Then, for any arbitrary $d \in \mathcal{D}$, the elements of the observation vectors, i.e. $y^{(n)}[k]$, are uncorrelated random variables. Moreover, the elements with an actual index difference greater than n_h are independent.*

Corollary 0.1. *Samples from different observation vectors are independent.*

According to Lemma 0.1, although the elements of the observation vectors, i.e. $y^{(n)}[k]$, are uncorrelated, and those with actual index difference greater than n_h are independent, but, they are not generally independent. Hence, deriving a closed-form expression for the joint PDF, i.e. $f(\mathbf{y}^{(0)}, \mathbf{y}^{(1)}, \dots, \mathbf{y}^{(N-1)} | H_d)$, is not mathematically tractable. However, authors in [16] showed that the final estimator is less sensitive to the independency assumption of the elements of the observation vectors than their sole PDFs. Thus, using Corollary 0.1, we can write

$$\begin{aligned} f(\mathbf{y}^{(0)}, \mathbf{y}^{(1)}, \dots, \mathbf{y}^{(N-1)} | H_d) &= f_{\mathbf{Y}^{(0)}}(\mathbf{y}^{(0)} | H_d) f_{\mathbf{Y}^{(1)}}(\mathbf{y}^{(1)} | \mathbf{y}^{(0)}, H_d) \dots \\ &\quad f_{\mathbf{Y}^{(N-1)}}(\mathbf{y}^{(N-1)} | \mathbf{y}^{(0)}, \mathbf{y}^{(1)}, \dots, H_d) \\ &= \prod_{n=0}^{N-1} f_{\mathbf{Y}^{(n)}}(\mathbf{y}^{(n)} | H_d) \\ &\simeq \prod_{n=0}^{N-1} \prod_{k=0}^{n_s-1} f_{Y^{(n)}[k]}(y^{(n)}[k] | H_d) \end{aligned} \quad (20)$$

Let us denote the in-phase and quadrature components of a received sample, i.e. $y^{(n)}[k]$, by $y_I^{(n)}[k]$ and $y_Q^{(n)}[k]$, respectively. Since, the in-phase and quadrature components are

independent from each other, one can rewrite Equation (20) as

$$\begin{aligned} f(\mathbf{y}^{(0)}, \mathbf{y}^{(1)}, \dots, \mathbf{y}^{(N-1)} | H_d) &\simeq \prod_{n=0}^{N-1} \prod_{k=0}^{n_s-1} f_{Y^{(n)}[k]}(y^{(n)}[k] | H_d) \\ &= \prod_{n=0}^{N-1} \prod_{k=0}^{n_s-1} f_{Y_I^{(n)}[k]}(y_I^{(n)}[k] | H_d) f_{Y_Q^{(n)}[k]}(y_Q^{(n)}[k] | H_d) \end{aligned} \quad (21)$$

Using Equation (15), we have $Y_I^{(n)}[k] = V_I^{(n)}[k] + W_I^{(n)}[k]$. The same equation holds for the quadrature components of the received samples. Hence, the PDF $f_{Y_I^{(n)}[k]}(y_I^{(n)}[k] | H_d)$, or similarly $f_{Y_Q^{(n)}[k]}(y_Q^{(n)}[k] | H_d)$, for $n \geq 0$ can be obtained as

$$\begin{aligned} f_{Y_I^{(n)}[k]}(y_I^{(n)}[k] | H_d) &= f_{V_I^{(n)}[k]}(v_I^{(n)}[k] | H_d) \\ &\quad * f_{W_I^{(n)}[k]}(w_I^{(n)}[k] | H_d) \end{aligned} \quad (22)$$

where $*$ denotes the convolution operation. Deriving the PDF $f_{V_I^{(n)}[k]}(v_I^{(n)}[k] | H_d)$, or $f_{V_Q^{(n)}[k]}(v_Q^{(n)}[k] | H_d)$, is complex, and results in a complicated expression [16]. Here, we approximate this PDF with a Gaussian PDF with zero mean and a specific variance for each received sample in favor of reducing the complexity of the final estimator. We later justify this assumption in more details.

The first step to derive the PDF of in-phase component of a received sample $Y_I^{(n)}[k]$ is to determine the corresponding mean and variance of $V_I^{(n)}[k]$ under assumption H_d . In the absence of TO, i.e. H_0 , Equation (15) holds and can be expanded as Equation (27) given at the top of the next page.

Using Equations (27) and (12) and the fact that $\mathbb{E}\{h_I[k]\} = \mathbb{E}\{h_Q[k]\} = 0$, we conclude

$$\mathbb{E}\{V_I^{(n)}[k] | H_0\} = 0. \quad (23)$$

By substituting

$$\begin{aligned} \mathbb{E}\{s_{I^2}^{(n)}[k]\} &= \mathbb{E}\{s_{Q^2}^{(n)}[k]\} \\ &= \begin{cases} \frac{\sigma_x^2}{2}, & 0 \leq k \leq n_x - 1 \\ 0, & n_x \leq k \leq n_s - 1 \end{cases} \end{aligned} \quad (24)$$

and $\mathbb{E}\{h_I^{(n)}[k]h_I^{(n)}[r]\} = \mathbb{E}\{h_Q^{(n)}[k]h_Q^{(n)}[r]\} = \sigma_{h_k}^2 \delta[k - r]$, and using Equation (27), one can derive

$$\begin{aligned} \sigma_k^2 &\triangleq \mathbb{E}\{(v_I^{(n)}[k])^2 | H_0\} \\ &= \begin{cases} \sum_{r=a}^b \frac{\sigma_{h_r}^2 \sigma_x^2}{2} & 0 \leq k < n_x + n_h - 2 \\ 0 & n_x + n_h - 1 \leq k \leq n_s - 1 \\ & \text{or } n < 0 \end{cases} \end{aligned} \quad (25)$$

where

$$(a, b) = \begin{cases} (0, k) & 0 \leq k \leq n_h - 2 \\ (0, n_h - 1) & n_h - 1 \leq k \leq n_x - 1 \\ (k - n_x + 1, n_h - 1) & n_x \leq k \leq n_x + n_h - 2. \end{cases} \quad (26)$$

$$v_1^{(n)}[k] = \begin{cases} \sum_{u=0}^m h_I[u]s_I^{(n)}[k-u] - h_Q[u]s_Q^{(n)}[k-u] & 0 \leq k < n_h - 2 \\ \sum_{u=0}^{n_h-1} h_I[u]s_I^{(n)}[k-u] - h_Q[u]s_Q^{(n)}[k-u] & n_h - 1 \leq k \leq n_x - 1, \\ \sum_{u=m-n_x+1}^{n_h-1} h_I[u]s_I^{(n)}[k-u] - h_Q[u]s_Q^{(n)}[k-u] & n_x \leq k \leq n_x + n_h - 2, \\ 0 & n_x + n_h - 1 \leq k \leq n_s - 1, \end{cases} \quad (27)$$

Using Equations (25) and (26), one can define the vector of variances of the received samples under assumption H_0 as $\sigma_{\mathbf{V}_1|H_0}^2 \triangleq$

$$\begin{bmatrix} \vdots \\ \sigma_{\mathbf{V}_1[-2]|H_0}^2 \\ \sigma_{\mathbf{V}_1[-1]|H_0}^2 \\ \hline \sigma_{\mathbf{V}_1[0]|H_0}^2 \\ \sigma_{\mathbf{V}_1[1]|H_0}^2 \\ \vdots \\ \sigma_{\mathbf{V}_1[n_s-1]|H_0}^2 \\ \hline \sigma_{\mathbf{V}_1[n_s]|H_0}^2 \\ \sigma_{\mathbf{V}_1[n_s+1]|H_0}^2 \\ \vdots \\ \sigma_{\mathbf{V}_1[c_1+2n_s-1]|H_0}^2 \\ \hline \vdots \end{bmatrix} \stackrel{(a)}{=} \begin{bmatrix} \vdots \\ 0 \\ 0 \\ \hline \sigma_0^2 \\ \sigma_1^2 \\ \vdots \\ \sigma_{n_s-1}^2 \\ \hline \sigma_0^2 \\ \sigma_1^2 \\ \vdots \\ \sigma_{n_s-1}^2 \\ \hline \vdots \end{bmatrix} \quad (28)$$

where $\sigma_{\mathbf{V}_1|H_0}^2[k] = \sigma_{\mathbf{V}_1[k]|H_0}^2$ corresponds to the variance of the k -th received sample under H_0 , i.e. $Y_1^{(n)}[k]$.

Now, note that any TO in the received samples of length m results in an only a shift in the vector of variances given in (28) as

$$\sigma_{\mathbf{V}_1|H_d}^2 = \sigma_{\mathbf{V}_1|H_0}^2(d : d + m - 1) \quad (29)$$

where we denote a shortened version of an arbitrary unlimited-length vector $\mathbf{a} = [\cdots a[-2] a[-1] a[0] a[1] a[2] \cdots]^T$ by $\mathbf{a}(r : k)$, $r \leq k$, and is defined as

$$\mathbf{a}(r : k) \triangleq [a[r] a[r+1] \cdots a[k]]^T. \quad (30)$$

Finally, using Equations (29) and (23), we have

$$V_1^{(n)}[k] \sim \mathcal{N}(0, \sigma_{\mathbf{V}_1|H_d}^2[k]), \quad (31)$$

where $V_1^{(n)}[k] \sim \mathcal{N}(0, 0)$ means $V_1^{(n)}[k] = 0$. Similar equation holds for $V_Q^{(n)}[k]$.

Now that we derived the variance of $V_1^{(n)}[k]$ under assumption H_d , i.e. Eq. (29), we are ready to derive the PDF of an

in-phase component of a received sample $Y_1^{(n)}[k]$ under H_d . Since $W^{(n)}[k] = W_1^{(n)}[k] + jW_Q^{(n)}[k]$, from (11) we have

$$f_{W_1^{(n)}[i]}(w) = \sum_{l=0}^{L-1} p_l \mathcal{CN}\left(w : 0, \frac{\sigma_{w_l}^2}{2}\right). \quad (32)$$

Finally, by substituting (31) and (32) into (22), we can write

$$\begin{aligned} f_{Y_1[k]}(y|H_d) &= \sum_{l=0}^{L-1} \frac{p_l}{\sqrt{2\pi\frac{\sigma_{w_l}^2}{2}}} \frac{1}{\sqrt{2\pi\sigma_{\mathbf{V}_1|H_d}^2[k]}} \times \\ &\int_{-\infty}^{\infty} \exp\left\{-\frac{1}{2\frac{\sigma_{w_l}^2}{2}}(y-v)^2\right\} \exp\left(-\frac{v^2}{2\sigma_{\mathbf{V}_1|H_d}^2[k]}\right) dv \\ &= \sum_{l=0}^{L-1} \frac{p_l \exp\left(-\frac{y^2}{\sigma_{w_l}^2}\right)}{\sqrt{2\pi\frac{\sigma_{w_l}^2}{2}}} \frac{1}{\sqrt{2\pi\sigma_{\mathbf{V}_1|H_d}^2[k]}} \\ &\int_{-\infty}^{\infty} \exp\left\{-\left(\frac{1}{\sigma_{w_l}^2} + \frac{1}{2\sigma_{\mathbf{V}_1|H_d}^2[k]}\right)v^2 + \left(\frac{2y}{\sigma_{w_l}^2}\right)v\right\} dv \\ &\stackrel{a}{=} \sum_{l=0}^{L-1} \frac{p_l}{\sqrt{2\pi(\sigma_{\mathbf{V}_1|H_d}^2[k] + \frac{\sigma_{w_l}^2}{2})}} \exp\left(-\frac{y^2}{2(\sigma_{\mathbf{V}_1|H_d}^2[k] + \frac{\sigma_{w_l}^2}{2})}\right) \end{aligned} \quad (33)$$

one can derive the similar equations for $f_{Y_Q[k]}(y|H_0)$.

Before we dig into the last step and derive the PDF of $Y^{(n)}[k]$, we use the next definitions to simplify notations.

Definition 1: The mathematical function $B(z, t) : \mathbb{R} \times \mathbb{R} \mapsto \mathbb{R}$ is defined as

$$B(z, t) = \sum_{l=0}^{L-1} \frac{p_l}{\sqrt{2\pi(t + \frac{\sigma_{w_l}^2}{2})}} \exp\left(-\frac{z^2}{2(t + \frac{\sigma_{w_l}^2}{2})}\right), \quad (34)$$

where $t \geq 0$.

Definition 2: The mathematical function $\mathcal{P}(c, \kappa) : \mathbb{C} \times \mathbb{R} \mapsto \mathbb{R}$ is called \mathcal{P} -function, and is defined as

$$\mathcal{P}(c, \kappa) = B(c_1, \kappa)B(c_2, \kappa), \quad (35)$$

where $c_1 = \text{Re}\{c\}$, $c_2 = \text{Im}\{c\}$, and $\kappa \geq 0$ is called shape parameter.

Using *Definitions 1* and *2* and Equation (33), one can show that the PDF of the received samples under H_d , i.e. $f_{Y[k]}(y|H_d)$, are \mathcal{P} -functions with different shape parameters as

$$\begin{aligned} f_{Y[k]}(y|H_d) &= f_{Y_1[k]}(y_I|H_d)f_{Y_Q[k]}(y_Q|H_d) \\ &= B(y_I, \sigma_{\mathbf{V}_1|H_d}^2[k])B(y_Q, \sigma_{\mathbf{V}_1|H_d}^2[k]) \\ &= \mathcal{P}(y, \sigma_{\mathbf{V}_1|H_d}^2[k]), \end{aligned} \quad (36)$$

where $y_I = \text{Re}\{y\}$, $y_Q = \text{Im}\{y\}$.

Finally, for any arbitrary number of received samples $m \geq 1$, i.e. $\mathbf{y} = [y[0] \ y[1] \ \cdots \ y[m-1]]^T$, using (36), we have

$$\begin{aligned} \hat{\mathbf{d}}^{\text{opt}} &= \underset{d \in \mathcal{D}}{\text{argmax}} \prod_{k=0}^{m-1} f_{Y[k]}(\mathbf{y}[k] | \mathbf{H}_d) \\ &= \underset{d \in \mathcal{D}}{\text{argmax}} \prod_{k=0}^{m-1} \mathcal{P}(\mathbf{y}[k], \sigma_{\mathbf{V}_I | \mathbf{H}_d}^2[k]). \end{aligned} \quad (37)$$

The next theorem summarizes our discussions in this section.

Theorem 1. *In a doubly selective channel and under impulsive noise defined in (11), the approximate NDA ML TO estimator for a ZP-OFDM systems is given as*

$$\hat{\mathbf{d}}^{\text{opt}} = \underset{d \in \mathcal{D}}{\text{argmax}} \prod_{k=0}^{m-1} \mathcal{P}(\mathbf{y}[k], \sigma_{\mathbf{V}_I | \mathbf{H}_d}^2[k]). \quad (38)$$

where $\mathcal{P}(c, \kappa)$ is defined in (35) and $\sigma_{\mathbf{V}_I | \mathbf{H}_d}^2[k]$ is given in (29).

A. Higher Order Statistical Analysis

In order to see that the Gaussian approximation of $V_I^{(n)}[k]$, or $V_Q^{(n)}[k]$, is mainly valid, we have plotted the true PDF of $Y_I^{(n)}[k]$ versus the approximate PDF given in (33) in Fig. 1 for different values of $k = 1$, chosen from the first range given in (27), and $k = 150$, chosen from the second range in (27). Moreover, the corresponding probabilistic measures such as mean, variance, skewness, and kurtosis of the true and approximate PDFs are given in Table I. Skewness measures the asymmetry of a probability distribution around its mean, and is defined as

$$sk \triangleq \frac{\mathbb{E}\{(Y - \mu)^3\}}{\mathbb{E}\{(Y - \mu)^2\}^{3/2}}. \quad (39)$$

Kurtosis is a measure of sharpness of a PDF, and is defined as

$$ku \triangleq \frac{\mathbb{E}\{(Y - \mu)^4\}}{(\mathbb{E}\{(Y - \mu)^2\})^2}. \quad (40)$$

The true PDF is obtained through 10^6 Monte Carlo simulations where $n_x = 512$, $n_z = 20$, $n_h = 10$, $f_s = 10^6$, and modulation order is $M = 128$. Also, an exponential power delay profile is considered and is given as

$$\mathbb{E}\{|h[k]|^2\} = \sigma_{h_k}^2 = \alpha \exp(-\beta k), \quad k = 0, 1, \dots, 9, \quad (41)$$

where $\alpha = 0.396$ is a normalizing factor that guarantees the average energy of the channel taps sum to one, and $\beta = 0.5$. For the sake of simplicity in illustrations, we set $p_0 = 1$, and $p_l = 0$, $\forall l \neq 0$, which resembles a Gaussian noise.

As can be seen in Fig. 1(a), when $k = 1$, the approximate PDF deviates from the true PDF in terms of Kurtosis, the sharpness of the PDF, and almost matches the other metrics such as skewness and variance. This deviation holds for the

TABLE I: Various probability measures for empirical PDF versus analytical PDF.

	$k = 1$		$k = 150$	
	Empirical	Analytical	Empirical	Analytical
Mean	-0.00022	0	0.00041	0
Variance	0.1231	0.1232	0.5021	0.5023
Skewness	-0.0048	0	0.0090	0
Kurtosis	4.4519	3	3.3000	3

samples in the first and third ranges given in (27) for the given setup, i.e. $0 \leq k \leq n_h - 2$ and $n_x \leq k \leq n_x + n_h - 2$. However, as seen in Fig. 1(b), when $k = 150$, the approximate PDF reasonably matches with the true PDF in terms of all probabilistic measures given in Table I. This approximate matching holds for the second and fourth ranges given in (27) for the given setup, i.e. $n_h - 1 \leq k \leq n_x - 1$ and $n_x + n_h - 1 \leq k \leq n_s - 1$. These ranges contain $\frac{n_x + n_z - 2n_h + 2}{n_x + n_z}$ of the samples in a given received OFDM vector which is more than 96% of the samples. That is, the approximate PDF reasonably matches the true PDF of more than 95% of the samples in a given received OFDM vector while it slightly differs for less than 5% of the received samples. This implies that the performance of the final estimator should not degrade considerably; although, the final estimator should have significantly lower complexity compared to that of given in [16] due to the simplicity of the approximate PDF.

B. Case Study: Gaussian noise when $d \geq 0$

Assume the receiver starts late to receive the samples. That is $d \geq 0$. Also, assume the receiver uses N vectors of n_s samples in order to estimate the TO in an environment with Gaussian noise. Taking logarithm of (37), and after some mathematical manipulations, we have

$$\hat{\mathbf{d}}^{\text{opt}} = \underset{d \in \mathcal{D}}{\text{argmin}} \sum_{k=0}^{N n_s - 1} \frac{|\mathbf{y}[k]|^2}{\sigma_{\mathbf{V}_I | \mathbf{H}_d}^2[k] + \frac{\sigma_{w_I}^2}{2}}. \quad (42)$$

Equation (42) shows that the final estimator in the given setup turns into a Weighted Energy Detector (WED). Note that WED assigns larger weights to those samples carrying no information, i.e. noise samples, while dedicating smaller weights to those carrying information.

C. Energy Detector

Inspired by WED derived in (42), we introduce a sub-optimal lower complexity estimator, i.e. ED, where we consider an extreme case of WED. That is, we assign a very large weight, i.e. one, to noise samples while we assign a zero weight to those samples carrying information. Hence,

$$\hat{\mathbf{d}}^{\text{opt}} = \underset{d \in \mathcal{D}}{\text{argmin}} \sum_{r=0}^{N-1} \sum_{k=\phi_1(d)}^{\phi_2(d)} |\mathbf{y}[k]|^2, \quad (43)$$

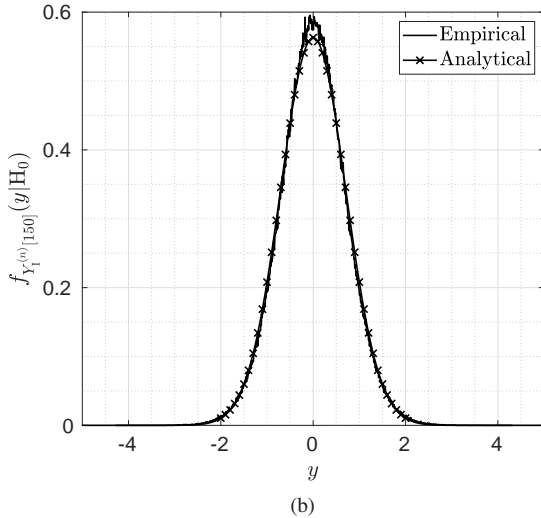
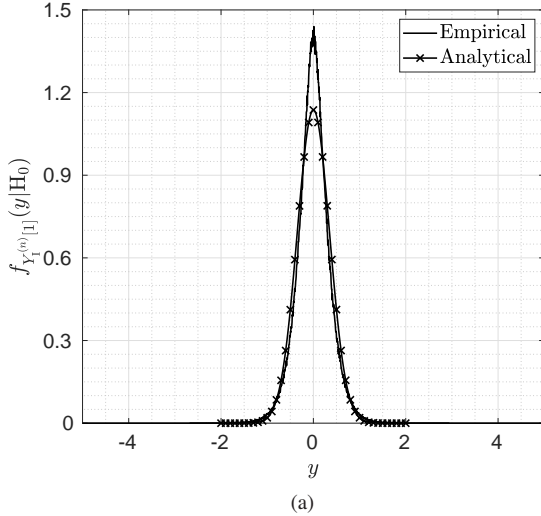


Fig. 1: The comparison between the empirical and analytical PDFs of the received samples for $k = 1$ and $k = 150$ when SNR= 15 dB.

where

$$\phi_1(d) \triangleq n_x + n_h - 1 + rn_s - d \quad (44)$$

$$\phi_2(d) \triangleq (r + 1)n_s - 1 - d. \quad (45)$$

In the next section, we extend the ML TO estimator given in Equation (37) for SISO systems to an ML TO estimator for MIMO systems.

D. Maximum Likelihood Estimation for Multiple-Input Multiple-Output System

In this subsection, we derive the ML TO for a MIMO-OFDM system under a frequency selective channel. We use the results proposed for SISO scenario, and try to extend the

notations. The next theorem gives ML TO estimator for MIMO systems.

Theorem 2. For a ZP MIMO-OFDM wireless communication system and Class A impulsive noise defined in (11), the approximate ML TO estimator is given as

$$\hat{\mathbf{d}}^{opt} = \underset{d \in \mathcal{D}}{\operatorname{argmax}} \prod_{j=1}^{m_r} \prod_{k=0}^{m-1} \mathcal{P}(\mathbf{y}_j[k], \sigma_{\mathbf{V}_1|H_d}^2[k]). \quad (46)$$

where $\mathcal{P}(c, \kappa)$ is defined in (35) and $\sigma_{\mathbf{V}_1|H_d}^2[k]$ is given in (29).

Proof: Using Equations (4), (5) and (7) for a MIMO-OFDM system, we have

$$\mathbf{y}_j^{(n)} = \sum_{i=1}^{m_t} \mathbf{H}_{ji}^{(n)} \mathbf{s}_i^{(n)} + \mathbf{w}_j^{(n)}, \quad \forall j \in \{1, 2, \dots, m_r\}. \quad (47)$$

Also, we have

$$\begin{aligned} \mathbb{E}\{s_i^{(n)}[k]s_p^{(n)}[k']^*\} &= \mathbb{E}\{x_i^{(n)}(kT_{sa})x_p^{(n)}(k'T_{sa})^*\} \quad (48) \\ &= \frac{\sigma_x^2}{m_t} \delta[k - k'] \delta[i - p], \\ &\quad \forall i, p \in \{1, 2, \dots, m_t\}, \\ &\quad \forall k, k' \in \{0, 1, \dots, n_x - 1\}. \end{aligned}$$

since the transmit power should remain the same for SISO and MIMO systems. Using (47) and following the same steps as in SISO case, one can arrive at (46). ■

Next section compares the complexity of the proposed approximate ML algorithm with that of given in [16].

IV. COMPLEXITY

Complexity of an algorithm plays a crucial role in using the algorithm in wireless communication systems. That is, an algorithm should be rather simple yet accurate enough in order to be considered for practical implementations. To this end, the complexity of the proposed approximate ML algorithm, referred to as A-ML, with the complexity of the original ML estimator in [16], denoted as O-ML, and that of Transition Metric [15] are given in Table II. As can be seen, A-ML has significantly lower computational complexity compared to O-ML while possessing a negligible performance loss in terms of lock-in probability, shown in next section. Also, A-ML has the same computational complexity as Transition Metric while demonstrating a large performance gap in terms of lock-in probability.

As seen, the main advantage of A-ML is its simplicity which enables the designer to easily extend it to MIMO systems. Note that A-ML can be implemented in fully vectorized format that makes it considerably faster than O-ML. One can further improve the complexity and the exhaustive search in (46) by using complexity-reduced search algorithms such as Golden Section Search algorithm which has a significantly lower complexity of $\mathcal{O}(\log(|\mathcal{D}|))$ compared to that of exhaustive search, $\mathcal{O}(|\mathcal{D}|)$.

TABLE II: Complexity of the proposed algorithms

Estimator	Computational Complexity
A-ML	$\mathcal{O}(Nn_s)$
O-ML	$\mathcal{O}(Nn_s^3)$
Transition Metric	$\mathcal{O}(Nn_s)$

V. SIMULATIONS

In this section, we compare the proposed algorithm A-ML with O-ML given in [16], and Transition Metric [15].

A. Simulation Setup

Unless otherwise mentioned, the following setup is considered for simulations. A ZP-OFDM system with 128-QAM modulation in a frequency-selective Rayleigh fading channel is considered with data samples length of $n_x = 512$, and ZP guard interval of length $n_z = 20$. The number of received OFDM vectors used for estimation is set $N = 10$. Sampling rate is $f_s = 10^6$. The exponential channel delay profile parameters are $\alpha = 1, \beta = 0.05$, where $n_h = 10$. A Jakes model for Doppler spectrum with maximum Doppler shift of $f_D = 5$ Hz is considered. A two-components impulsive noise with parameters $p_0 = 0.99, p_1 = 0.01, \sigma_{w_0}^2 = 1$, and $\sigma_{w_1}^2 = 100$ is set. SNR in dB is defined as $\gamma \triangleq 10 \log(\frac{\sigma_x^2}{\sigma_w^2})$. Simulation results are obtained through 10^4 Monte Carlo realizations, and the delay is uniformly chosen from the range $d \in [-30, 30]$.

B. Simulation Results

The probability of lock-in of A-ML, O-ML and Transition Metric for different values of SNR when $m_t = m_r = 1$ are depicted in Fig. 2. As shown, there is a negligible performance gap between A-ML and O-ML while A-ML possesses a much lower computational complexity. Also, A-ML significantly outperforms Transition Metric.

The performance of A-ML versus the number of observation vectors used for estimation is shown in Fig. 3. As seen, the performance of A-ML improves as the number of observation vectors increases. This figure shows that with a reasonable buffer capacity or an increase in the number of antennas, a receiver using A-ML is able to achieve high lock-in probability, e.g. more than 0.9.

The performance of WED and ED for different values of positive delays, i.e. when the receiver starts late to receive samples, and for various SNR values is depicted in Fig. 4. This figure shows that ED is able to achieve a high probability of lock-in in higher SNRs while a considerable performance gap is clear at lower SNRs. This performance gap is originating from the simplifying assumption of zero and one weight assignments in ED, which results in significantly lower computational complexity of ED compared to WED.

Fig. 5 shows the performance of A-ML for MIMO systems for different values of m_t and m_r . As seen, the performance of A-ML improves significantly due to the fact that the number

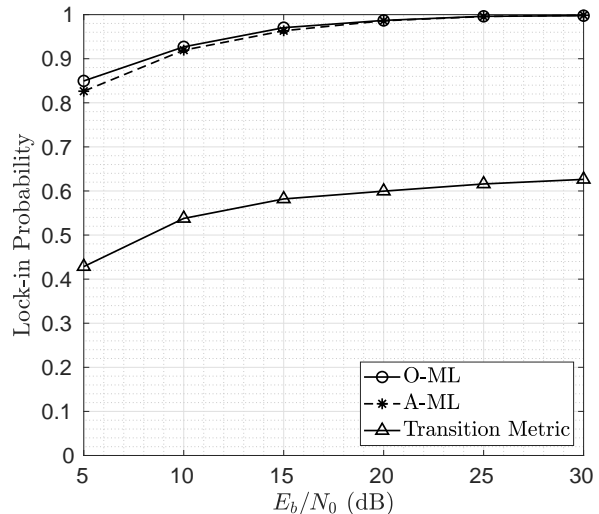


Fig. 2: Lock-in probability of A-ML, O-ML and Transition Metric for different values of SNR.

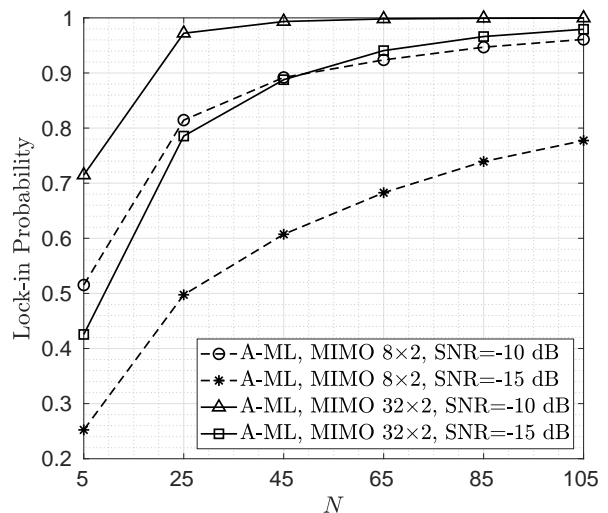


Fig. 3: Lock-in probability of A-ML for different number of observation vectors used for estimation.

of receive samples used for estimation increases when the number of transmit or receive antenna increases. Increasing the number of observations improves the accuracy of ML estimators; hence, the performance of A-ML improves.

The effect of impulsive noise on the performance of A-ML is shown in Fig. 6. Here, we consider a two-components Gaussian mixture where $\sigma_{w_0}^2 = 1, \sigma_{w_1}^2 = 100$, and we change the ratio of p_0/p_1 . As seen, when a component, i.e. $\sigma_{w_0}^2 = 1$, becomes strong, i.e. p_0 increases, the performance improves. This is because the uncertainty of A-ML arising from Eq. (33) decreases as p_0 increases.

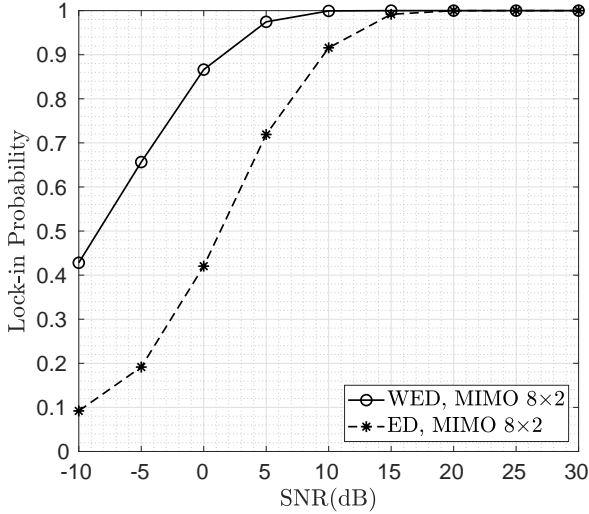


Fig. 4: Lock-in probability of WED and ED for values of SNR.

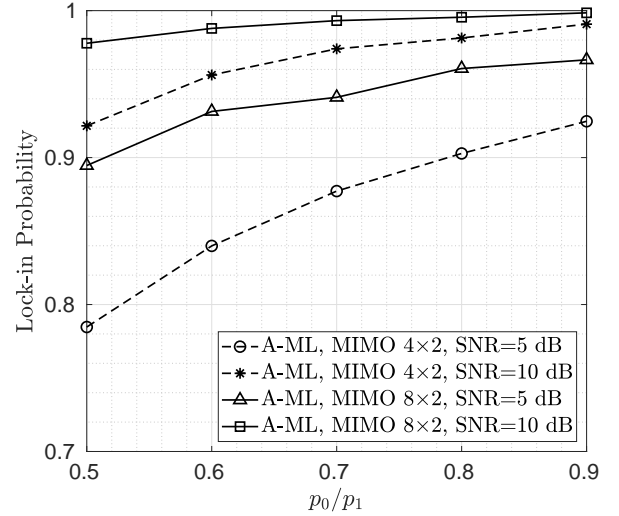


Fig. 6: Lock-in probability of A-ML for different values of p_0/p_1 .

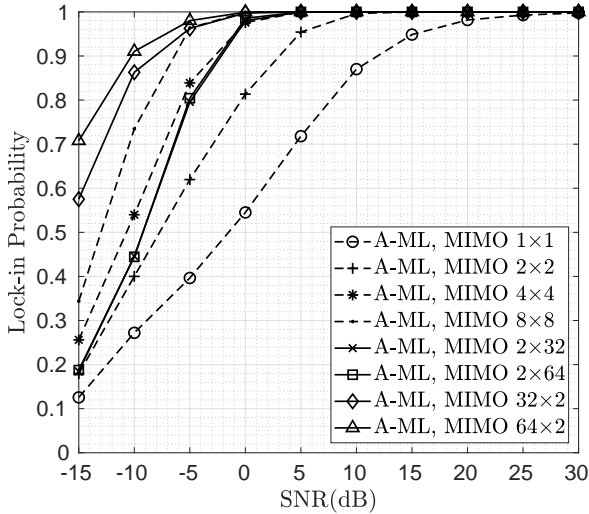


Fig. 5: Lock-in probability of A-ML for various number of antennas.

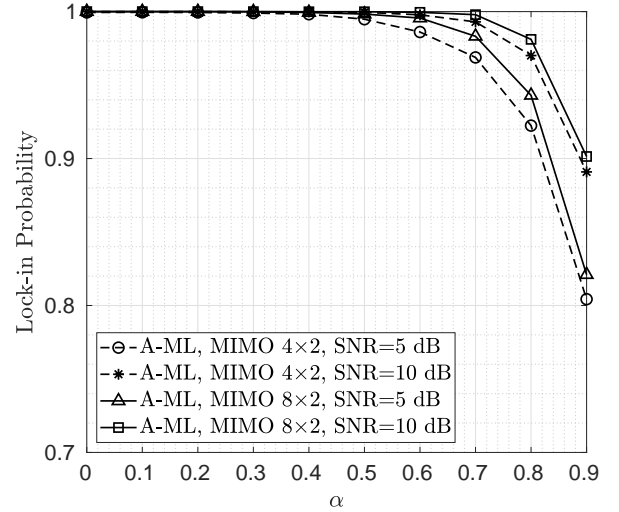


Fig. 7: Lock-in probability of A-ML for different values of power delay profile estimation errors.

Since A-ML employs power delay profile for synchronization, we study the sensitivity of A-ML to power delay profile estimation errors in Fig. 7. In order to generate power delay profile errors, we use the following equation

$$\sigma_{h_k}^2 = (1 + A_k \alpha) \sigma_{h_k}^2, \quad k = 0, 1, \dots, n_h - 1, \quad (49)$$

where A_k is uniformly (randomly) chosen for each tap from the set $\{-1, 1\}$. $\sigma_{h_k}^2$, instead of $\sigma_{h_k}^2$, is then fed to A-ML in order to estimate TO. The probability of lock-in of A-ML for different values of α is shown in Fig. 7. Although the performance of A-ML degrades with an increase in power delay profile error; however, a large error is required to achieve a 50% loss in terms of lock-in probability. Moreover, note that

an error of 0.7 results in less than four percent performance loss which implies that A-ML is fairly insensitive to power delay profile estimation errors.

VI. CONCLUSION

ZP-OFDM systems possess many advantages compared to CP-OFDM systems. However, the time synchronization in ZP-OFDM systems are significantly challenging due to the lack of CP. In this paper, we proposed an approximate yet accurate low-complexity NDA ML TO estimator, i.e. A-ML, for ZP MIMO-OFDM systems in highly selective channels. We showed that A-ML has a significantly lower complexity than

that of proposed in [16], i.e. O-ML, while having a negligible performance gap in terms of lock-in probability. This makes A-ML, unlike O-ML, suitable for practical implementations. Moreover, it is shown that A-ML dramatically outperforms the current state-of-the-art NDA TO estimator for ZP-OFDM referred to as Transition Metric.

REFERENCES

- [1] B. Lu and X. Wang, "Space-time code design in ofdm systems," in *Proc. IEEE GLOBECOM*, vol. 2, San Francisco, CA, USA, 2000, pp. 1000–1004.
- [2] L. Dai, Z. Wang, J. Wang, and Z. Yang, "Positioning with OFDM signals for the next-generation GNSS," *IEEE Trans. Consum. Electron.*, vol. 56, no. 2, pp. 374–379, May 2010.
- [3] C. D. Murphy, "Low-complexity FFT structures for OFDM transceivers," *IEEE Trans. Commun.*, vol. 50, no. 12, pp. 1878–1881, Dec. 2002.
- [4] S. Huang and S. Chen, "A green FFT processor with 2.5-GS/s for IEEE 802.15.3c (WPANs)," in *Proc. ICGCS*, Shanghai, China, Jun. 2010, pp. 9–13.
- [5] V. P. G. Jimenez, M.-G. Garcia, F. G. Serrano, and A. G. Armada, "Design and implementation of synchronization and AGC for OFDM-based WLAN receivers," *IEEE Trans. Consum. Electron.*, vol. 50, no. 4, pp. 1016–1025, Nov. 2004.
- [6] M. Kim and S. Chang, "A consumer transceiver for long-range IoT communications in emergency environments," *IEEE Trans. Consum. Electron.*, vol. 62, no. 3, pp. 226–234, Aug. 2016.
- [7] S.-G. Kim, H.-S. Kim, and S.-H. Park, "Apparatus and method for receiving digital multimedia broadcasting in a wireless terminal," Oct. 21 2008, US Patent 7,440,516.
- [8] D. C. Alves, G. S. da Silva, E. R. de Lima, C. G. Chaves, D. Urdaneta, T. Perez, and M. Garcia, "Architecture design and implementation of key components of an OFDM transceiver for IEEE 802.15.4g," in *Proc. IEEE ISCAS*, Montreal, QC, Canada, May 2016, pp. 550–553.
- [9] X. Wang, P. Ho, and Y. Wu, "Robust channel estimation and ISI cancellation for OFDM systems with suppressed features," *IEEE J. Sel. Areas Commun.*, vol. 23, no. 5, pp. 963–972, May 2005.
- [10] S. Roy and C. Li, "A subspace blind channel estimation method for OFDM systems without cyclic prefix," *IEEE Trans. Wireless Commun.*, vol. 1, no. 4, pp. 572–579, Oct. 2002.
- [11] F. Tufvesson, O. Edfors, and M. Faulkner, "Time and frequency synchronization for OFDM using PN-sequence preambles," in *Gateway to 21st Century Communications Village. in Proc. IEEE VTC*, vol. 4, The Netherlands, Fall 1999, pp. 2203–2207.
- [12] B. Muquet, M. de Courville, G. B. Giannakis, Z. Wang, and P. Duhamel, "Reduced complexity equalizers for zero-padded OFDM transmissions," in *Proc. IEEE ICASSP*, Istanbul, Turkey, 2000, pp. 2973–2976.
- [13] A. A. Nasir, S. Durrani, H. Mehrpouyan, S. D. Blostein, and R. A. Kennedy, "Timing and carrier synchronization in wireless communication systems: a survey and classification of research in the last 5 years," *EURASIP Journal on Wireless Communications and Networking*, no. 1, p. 180, Dec. 2016.
- [14] H. Bolcskei, "Blind estimation of symbol timing and carrier frequency offset in wireless OFDM systems," *IEEE Trans. Commun.*, vol. 49, no. 6, pp. 988–999, Jun. 2001.
- [15] V. Le Nir, T. van Waterschoot, J. Duplity, and M. Moonen, "Blind coarse timing offset estimation for CP-OFDM and ZP-OFDM transmission over frequency selective channels," *EURASIP Journal on Wireless Communications and Networking*, vol. 2009, no. 1, p. 262813, Jan. 2010. [Online]. Available: <https://doi.org/10.1155/2009/262813>
- [16] M. A. K.P. Roshandeh, M. MohammadKarimi, "Maximum likelihood time synchronization for zero-padded ofdm," *submitted to IEEE Trans. Signal Process.*
- [17] K. L. Blackard, T. S. Rappaport, and C. W. Bostian, "Measurements and models of radio frequency impulsive noise for indoor wireless communications," *IEEE J. Sel. Areas Commun.*, vol. 11, no. 7, pp. 991–1001, Sept. 1993.
- [18] D. Middleton, "Man-made noise in urban environments and transportation systems: Models and measurements," *IEEE Trans. Commun.*, vol. 21, no. 11, pp. 1232–1241, Nov. 1973.
- [19] D. Middleton and A. Spaulding, "Elements of weak signal detection in non-Gaussian noise," *Advances in Statistical Signal Processing*, vol. 2, pp. 137–215, 1993.
- [20] D. Middleton, "Channel modeling and threshold signal processing in underwater acoustics: An analytical overview," *IEEE Journal of Oceanic Engineering*, vol. 12, no. 1, pp. 4–28, Jan. 1987.
- [21] X. Wang and H. V. Poor, "Robust multiuser detection in non-Gaussian channels," *IEEE Trans. Signal Process.*, vol. 47, no. 2, pp. 289–305, Feb. 1999.
- [22] T. Shongwe, A. H. Vinck, and H. C. Ferreira, "A study on impulse noise and its models," *SAIEE Africa Research Journal*, vol. 106, no. 3, pp. 119–131, Sept. 2015.